

# Generalised parton distributions at HERA and prospects for COMPASS

L. Schoeffel\*

*CEA/Saclay, DAPNIA/Service de physique des particules, 91191 Gif-sur-Yvette cedex, France*

We present a model of generalised parton distributions based on a forward ansatz in the DGLAP region. We discuss some aspects of the parametrisations, as the dependence in  $t$ , with factorised and non-factorised approaches, where  $t$  is the square of the four-momentum exchanged at the hadron vertex. The predictions of this model are then compared with DVCS cross sections from H1 and ZEUS, and a related observable, the skewing factor, defined as the following ratio imaginary amplitudes :  $R \equiv \left. \text{Im} \mathcal{A}(\gamma^* + p \rightarrow \gamma + p) \right|_{t=0} / \left. \text{Im} \mathcal{A}(\gamma^* + p \rightarrow \gamma^* + p) \right|_{t=0}$ . It is an interesting quantity including both the non-forward kinematics and the non-diagonal effects. Finally, we discuss the beam charge asymmetry, which is certainly the most sensitive observable to the different hypothesis needed in the GPDs parametrisations. We show that the approximations done for the  $t$  dependence lead to significant differences for the predictions in the HERMES kinematic domain and prospects are given for COMPASS.

## I. INTRODUCTION

Measurements of the deep-inelastic scattering (DIS) of leptons and nucleons,  $e + p \rightarrow e + X$ , allow the extraction of Parton Distribution Functions (PDFs) which describe the longitudinal momentum carried by the quarks, anti-quarks and gluons that make up the fast-moving nucleons. These functions have been measured over a wide kinematic range in the Bjorken scaling variable  $x_{Bj}$  and the photon virtuality  $Q^2$ . While PDFs provide crucial input to perturbative Quantum Chromodynamic (QCD) calculations of processes involving hadrons, they do not provide a complete picture of the partonic structure of nucleons. In particular, PDFs contain neither information on the correlations between partons nor on their transverse motion, then a vital knowledge about the three dimensional structure of the nucleon is lost. Hard exclusive processes, in which the nucleon remains intact, have emerged in recent years as prime candidates to complement this essentially one dimensional picture [1, 2, 3, 4, 5, 6, 7, 8, 9, 10, 11, 12, 13]. This missing information is then encoded in Generalised Parton Distributions (GPDs). These functions carry information on both the longitudinal and the transverse distribution of partons. The recent strong interest in GPDs was stimulated by their relation with the spin structure of the nucleon. Indeed, GPDs are so far the only known means of probing the orbital motion of partons in the nucleon through Ji's Sum Rule [1], which relates unpolarised GPDs to the total angular momentum of the proton.

The simplest process sensitive to GPDs is deeply virtual Compton scattering (DVCS) or exclusive production of real photon,  $e + p \rightarrow e + \gamma + p$ . This process is of particular interest as it has both a clear experimental signature and is calculable in perturbative QCD. Also, it does not suffer from the uncertainties caused by the lack of understanding of the meson wave function that plague exclusive vector meson electroproduction. The DVCS reaction can be regarded as the elastic scattering of the virtual photon off the proton via a colourless exchange, producing a real photon in the final state. In the Bjorken scaling regime, QCD calculations assume that the exchange involves two partons, having different longitudinal and transverse momenta, in a colourless configuration. These unequal momenta are a consequence of the mass difference between the incoming virtual photon and the outgoing real photon. The DVCS cross section depends, therefore, on GPDs [3, 4, 5, 6, 9, 10, 11, 12, 13].

The reaction  $e + p \rightarrow e + \gamma + p$  receives contributions from both the DVCS process, whose origin lies in the strong interaction, and the purely electromagnetic Bethe-Heitler (BH) process where the photon is emitted from the positron. Therefore, measurements can be done either of the DVCS cross section itself or of the interference between the DVCS and BH processes, accessible via asymmetries. Measurements of the DVCS cross section at high energy have been obtained by H1 [14, 15] and ZEUS [16] and the helicity asymmetry in DVCS has been measured at lower energy with polarised lepton beams (and unpolarised targets) by HERMES [17] and CLAS [18, 19]. Recently, lepton beam charge asymmetry have been measured by HERMES [20]. These last observables are very sensitive to the shape of the GPDs and give a good opportunity to pin-down their parametrisations. It is the goal of a future program at COMPASS [4, 21] to realise a dedicated measurement and to access the beam charge asymmetry under favorable conditions.

In this paper, we focus our study on the HERA results and we show that GPDs parametrisations based on the

---

\*Electronic address: laurent.schoeffel@cea.fr

model of Ref. [13] are well suited to describe all measurements in this range of  $x_{Bj}$  ( $x_{Bj} < 0.1$ ). In section II, we present the model. We show the predicted DVCS cross section compared to data in section III. In this section, we also extract the skewing factor from data and from the model. This factor is an interesting observable to illustrate the data/model comparison and the building of the skewedness. In section IV, we discuss the case of the beam charge asymmetry measured at HERMES and we give some prospects for COMPASS.

## II. MODEL OF GENERALISED PARTON DISTRIBUTIONS

As mentioned in the introduction, GPDs are an extension of the well-known parton distribution functions (PDFs) appearing in inclusive processes such as deep inelastic scattering (DIS), or Drell-Yan, and encode additional information about the partonic structure of hadrons, above and beyond that of conventional PDFs. As such, the GPDs depend on four variables  $(X, \zeta, Q^2, t)$  rather than just two  $(x_{Bj}, Q^2)$  as is the case for PDFs. We use the notations of Ref. [2], where the variable  $X$  is defined in the range  $[0, 1]$  and the variable  $\zeta$  defines the skewedness with  $\zeta \simeq x_{Bj}$ . This allows an extended mapping of the dynamical behavior of the nucleon in the two extra variables, the skewedness  $\zeta$ , and the four-momentum squared exchanged at the hadron vertex,  $t$ . In the following, we define GPDs at a starting scale  $Q_0^2$  and their  $Q^2$  evolution is generated by perturbative QCD [9, 10, 11, 12, 13]. They contain, in addition to the usual PDF-type information residing in the so-called ‘‘DGLAP region’’ (for which the momentum fraction variable is larger than the skewedness parameter,  $X > \zeta$ ), supplementary information about the distribution amplitudes of virtual ‘‘meson-like’’ states in the nucleon in the so-called ‘‘ERBL region’’ ( $X < \zeta$ ) [9]. The parametrisation of GPDs is then a complicated task as the degrees of freedom are much larger than for PDFs.

Concerning the  $X, \zeta$  dependences, we follow the model presented in Ref. [13], using a forward ansatz at the initial scale  $Q_0 = 1.3$  GeV for the DGLAP domain  $[\zeta, 1]$  :

$$H_S(X, \zeta) \equiv \frac{q_S \left( \frac{X - \zeta/2}{1 - \zeta/2} \right)}{1 - \zeta/2}, \quad (1)$$

where  $q_S$  refers to a singlet forward distribution [22] and  $H_S(X, \zeta) = H_q(X, \zeta) + H_{\bar{q}}(X, \zeta)$ . A similar relation holds for valence and gluon distributions. This Ansatz in the DGLAP region corresponds to a double distribution model with an extremal profile function allowing no additional skewedness except for the kinematical one. Concerning the ERBL domain, we follow the strategy of Ref. [13]. GPDs must be continuous at  $X = \zeta$  and verify correct symmetry relations at  $X = \zeta/2$ . Then, the singlet distribution can be parametrised as

$$H_S(X, \zeta) \equiv H_S(\zeta, \zeta) \frac{X - \zeta/2}{\zeta/2} [1 + A_S(\zeta) f(X, \zeta)] \quad (2)$$

where  $f(X, \zeta)$  is an even function of the variable  $X - \zeta/2$  such that  $f(\zeta, \zeta) = 0$  to ensure the continuity relation at  $X = \zeta$ . Thus, we can write :  $f(X, \zeta) \propto 1 - (X - \zeta/2)^2/(\zeta/2)^2$ . The parameters  $A_S(\zeta)$  are determined for each value of  $\zeta$  by requiring that the first momentum sum rule of the GPD is satisfied [1, 2]. All other GPDs are parametrised as exposed in Ref. [13]. The skewed QCD evolution code has been rewritten for the purpose of this paper.

Results are shown in Fig. 1 for the generalised  $u$  quark singlet density, for two values skewedness  $\zeta = 0.05$  and  $\zeta = 10^{-3}$ , at the initial scale and after a QCD evolution. We notice that the skewedness effect manifest itself much before the border between the DGLAP and ERBL domains at  $X = \zeta$ . In particular, for the lowest  $\zeta$  value of  $10^{-3}$ , the GPD follows exactly the PDF till  $X \simeq 10^{-2}$ , where the skewing effect starts to appear, as expected from the forward limit condition : GPDs are obliged to reproduce the PDFs in the forward limit  $\zeta \rightarrow 0$ , with  $H_{Us}(X, \zeta = 0) = Us(X) = u(X) + \bar{u}(X)$ . Also, we observe in Fig. 1 that the generalised  $u$  quark singlet distribution is antisymmetric at  $X = \zeta/2$  in the ERBL region and this property is preserved under evolution. In Fig. 2, we present the generalised gluon density again for two values skewedness  $\zeta = 0.05$  and  $\zeta = 10^{-3}$ , at the initial scale and after a QCD evolution. Here also, for the lowest  $\zeta$  value of  $10^{-3}$ , the GPD follows exactly the PDF till  $X \simeq 10^{-2}$  as expected from the forward limit condition  $H_G(X, \zeta = 0) = XG(X)$ .

Concerning the  $t$  dependence in the low  $x_{Bj}$  kinematic domain of H1 and ZEUS measurements [15], it has been shown that the DVCS cross section,  $d\sigma/dt$ , can be factorised and approximated by an exponential form  $e^{-b|t|}$ , implying a factorised dependence in  $e^{-b/2|t|}$  for GPDs. It follows from Ref. [15] that the measured  $t$ -slopes  $b$  present a  $Q^2$  dependence compatible with the form :  $b(Q^2) = A (1 - 0.15 \log(Q^2/2))$ , where  $A = 7.6 \pm 0.80$  GeV $^{-2}$ . We keep this expression in the following when describing H1 and ZEUS measurements, as it is done also in Ref. [11]. Of course, it can only be considered as an effective approximation of a more realistic non-factorised approach [8]. In Ref. [11], a non-factorised  $t$  dependence is proposed with a Regge motivated approach. In this approximation, we can write the

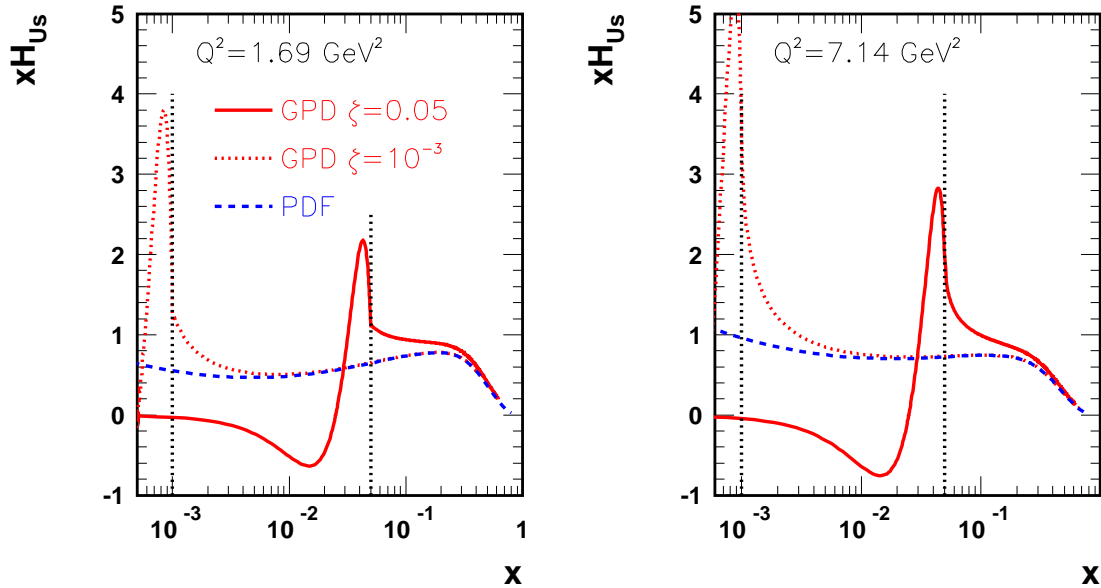


FIG. 1: The generalised distribution of the u quark singlet (multiplied by  $X$ )  $XH_{Us}(X, \zeta) = XH_u(X, \zeta) + XH_{\bar{u}}(X, \zeta)$  is presented for two values of the skewedness  $\zeta = 0.05$  and  $10^{-3}$ . The standard PDF  $XU_s(X) = Xu(X) + X\bar{u}(X)$  is also displayed. These functions are given at the initial  $Q_0^2$  value of  $1.69 \text{ GeV}^2$  (left) and after the NLO QCD evolution towards  $7.14 \text{ GeV}^2$  (right). In case of GPD, the evolution is done in the DGLAP and ERBL domain ensuring proper continuity relations at the border [13]. Two vertical lines at  $X = 0.05$  and  $X = 10^{-3}$ , corresponding to the skewing values, are also shown to indicate the position in  $X$  of the transition between the DGLAP and ERBL domains.

singlet distribution at the initial scale in the DGLAP domain :

$$H_S(X, \zeta, t; Q_0^2) \equiv \left[ \left( \frac{1 - \zeta/2}{X - \zeta/2} \right)^{\alpha'_S t} \right] \frac{q_S \left( \frac{X - \zeta/2}{1 - \zeta/2} \right)}{1 - \zeta/2},$$

with similar expressions for the gluon and valence distributions. This parametrisation is mixing the  $X$  and  $t$  dependences, thus it is labeled as non-factorised. It is inspired from Regge phenomenology as parameter  $\alpha'_S$  is characteristic of a Regge trajectory. We take the values :  $\alpha'_S = 0.9 \text{ GeV}^{-2}$  and  $\alpha'_g = 0.5 \text{ GeV}^{-2}$  as in Ref. [11].

In the next sections, we compare this model with the different approximations on the  $t$  dependence to available observables provided by H1, ZEUS and HERMES experiments.

### III. PREDICTIONS FOR THE DVCS CROSS SECTION AND RELATED OBSERVABLE

Using these parametrisations of GPDs at the initial scale  $Q_0 = 1.3 \text{ GeV}$ , calculated to higher  $Q^2$  values with a skewed QCD evolution, and assuming the  $t$  dependences described above, we can provide predictions for the DVCS cross section measurements. We present the results in Fig. 3 with H1 and ZEUS data [15, 16]. The measurements are integrated over  $t$  in the range  $[-1, 0] \text{ GeV}^2$ . Then, the model predictions are also integrated over the same range. Concerning these predictions, the uncertainty due to the limited knowledge of the  $t$ -slopes is displayed in Fig. 3. The calculations in the non-factorised  $t$  approach fall within this error, which shows that the DVCS cross sections are not sufficient to discriminate between these two hypothesis.

Also, a good agreement between data and the model predictions is observed : it shows that the simple description of the initial condition using a forward ansatz in the DGLAP domain and then generating the higher  $Q^2$  values from a skewed QCD evolution is a good approach. In particular, it can be noticed in Fig. 3 that the  $Q^2$  dependence of the DVCS cross section is well reproduced. The DVCS cross section follows a global  $1/Q^3$  shape, whose origin lies in

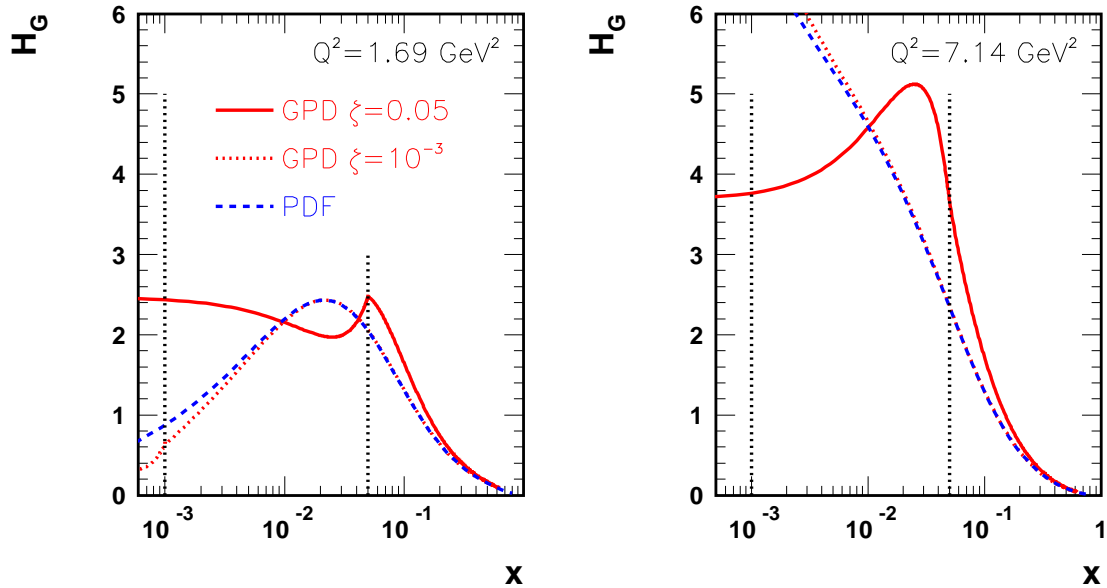


FIG. 2: The generalised distribution of the gluon  $H_G(X, \zeta)$  is presented for two values of the skewedness  $\zeta = 0.05$  and  $10^{-3}$ . The standard PDF  $XG(X)$  is also displayed. These functions are given at the initial  $Q_0^2$  value of  $1.69 \text{ GeV}^2$  (left) and after the NLO QCD evolution towards  $7.14 \text{ GeV}^2$  (right).

the product of the  $1/Q^4$  propagator of the virtual photon and the  $(Q^2)^\gamma$  behaviour of the GPDs implied by the QCD evolution, with the anomalous dimension  $\gamma \sim 0.5$ . The  $W$  dependence can be fitted by a form in  $W^\delta$  with  $\delta \simeq 0.7$ , a large exponent value characteristic of a hard QCD process [15, 16].

It is interesting to present the DVCS cross section measurements in a form which illustrates directly the skewing properties by defining a quantity which includes both the non-forward kinematics and the non-diagonal effects. Namely, we set the ratio between the imaginary parts of the DIS and DVCS (forward) scattering amplitudes at zero momentum transfer:

$$R \equiv \frac{\text{Im } \mathcal{A}(\gamma^* + p \rightarrow \gamma + p) \Big|_{t=0}}{\text{Im } \mathcal{A}(\gamma^* + p \rightarrow \gamma^* + p) \Big|_{t=0}}. \quad (3)$$

The virtual photon is assumed to be mainly transversely polarised in the case of DVCS process due to the real photon in the final state and has to be taken transversely polarised in the DIS amplitude also. The scattering amplitude for the DIS process can be obtained from the (transverse) DIS cross section [23], that is  $\text{Im } \mathcal{A}(\gamma^* p \rightarrow \gamma^* p) \sim \sigma_T(\gamma^* p \rightarrow X)$ . In fact, the DIS amplitude can be written using the usual pQCD fits for the transverse proton structure function,  $\sigma_T^{\gamma^* p} = (4\pi^2 \alpha_{EM}/Q^2) F_T^p(x, Q^2)$  and the DVCS scattering amplitude can be obtained from the recent measurements on the Deeply Virtual Compton Scattering cross section. We have shown that the DVCS cross sections are not sensitive to the hypothesis done on the  $t$  dependence described in section II. Then, obviously, the same conclusion holds for the skewing factor and we keep, for its determination, the effective approximation supported by the H1 data [15] that the  $t$  dependence of the amplitude can be factorised out and parameterised as an exponential. The total DVCS cross section can be related to the corresponding amplitude at  $t = 0$ :

$$\sigma(\gamma^* p \rightarrow \gamma p) = \frac{\left[ \text{Im } \mathcal{A}(\gamma^* p \rightarrow \gamma p) \Big|_{t=0} \right]^2}{16\pi b(Q^2)}, \quad (4)$$

where  $b(Q^2)$  is the  $t$ -slope function of  $Q^2$  described in section II. The expression above is corrected by taking into account the contribution from the real part of the amplitude by multiplying Eq. (4) by a factor  $(1 + \rho^2)$ , where  $\rho$  is

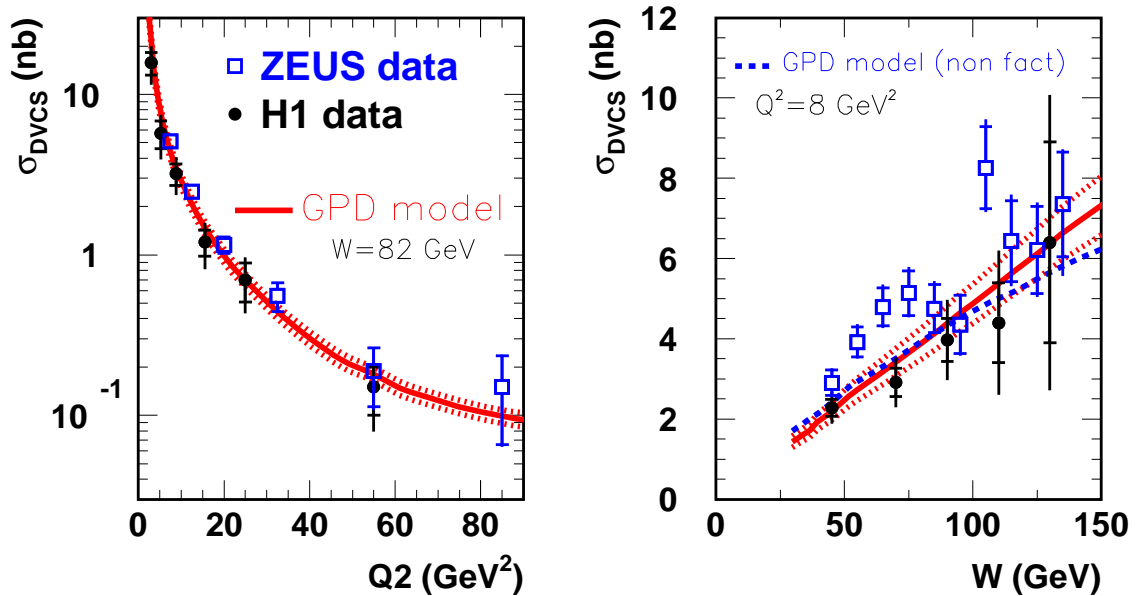


FIG. 3: DVCS cross section as a function of  $Q^2$  at  $W = 82 \text{ GeV}$  (left), and as a function of  $W$  at  $Q^2 = 8 \text{ GeV}^2$  (right). The GPD model predictions [13] are integrated over the  $t$  range of the measurements and displayed (see text). The model of section II, using an exponential factorised  $t$  dependence is shown with full lines on both the  $Q^2$  and  $W$  dependences of the DVCS cross section. The dotted lines illustrate the uncertainty on the  $t$ -slope dependence as described in section II. On the DVCS cross section as a function of  $W$ , we also display, as a dashed line, the model described in section II using a non-factorised  $t$  dependence (see text). The results of the factorised and non-factorised approaches are close and the differences are within the dotted lines. For clarity, we do not show the non-factorised curve on the  $Q^2$  dependence plot, as it would be very close to the factorised model on a logarithmic scale.

the ratio of the real to imaginary part of the DVCS amplitude. For the theory prediction, we use the real part of the DVCS amplitude as derived following the model of section II. To a good approximation,  $\rho$  can be calculated using dispersion relations to  $\rho \simeq \tan(\pi\lambda/2)$ , where  $\lambda = \lambda(Q^2)$  is the effective power of the Bjorken  $x_{Bj}$  dependence of the imaginary part of the amplitude. We use this property to correct the skewing factor extracted from the data. In this case, we estimate of the real part contribution by using the effective power for the inclusive deep inelastic reaction taken from Ref. [24]. The typical contribution for the kinematic window available at HERA is of the order of 10 %.

Considering the calculation discussed above, we can rewrite the skewing factor as a function of the cross sections for DIS ( $\sigma_T$ ) and DVCS :

$$R = \frac{4 \sqrt{\pi \sigma_{DVCS} b(Q^2)}}{\sigma_T(\gamma^* p \rightarrow X) \sqrt{(1 + \rho^2)}} = \frac{\sqrt{\sigma_{DVCS} Q^4 b(Q^2)}}{\sqrt{\pi^3 \alpha_{EM} F_T(x, Q^2) \sqrt{(1 + \rho^2)}}}, \quad (5)$$

Main theoretical uncertainties come from the  $t$ -slope,  $b(Q^2)$ , given in section II. Results are shown in Fig. 4, where a good data/model agreement is observed within errors.

On the skewing factor, we can exemplify the part of the skewing arising from the kinematic of the DVCS process and from the  $Q^2$  evolution itself. Then, we apply the forward ansatz, used at the initial scale 1.3 GeV in the model described in section II, at all values of  $Q^2$ . It means that we impose the parametrisation  $H_S(X, \zeta; Q^2) \equiv \frac{q_S(\frac{x-\zeta/2}{1-\zeta/2}; Q^2)}{1-\zeta/2}$  in the DGLAP domain for all values of  $Q^2$ , and similar relations for valence and gluon distributions. As illustrated in figure 4, the measurements show that such an approximation, which only takes into account the kinematical skewedness, is not sufficient to reproduce the total skewing effects generated by the QCD evolution equations.

In the limit when  $Q^2$  tends to zero, we also expect that the model should give a skewing factor equal to unity. We verify this point in Fig. 4 by propagating the calculations of  $R$  to very low values of  $Q^2$ . We observe that both the GPD model of section II and the pure forward model of section IV are converging to the same  $R = 1$  limit.

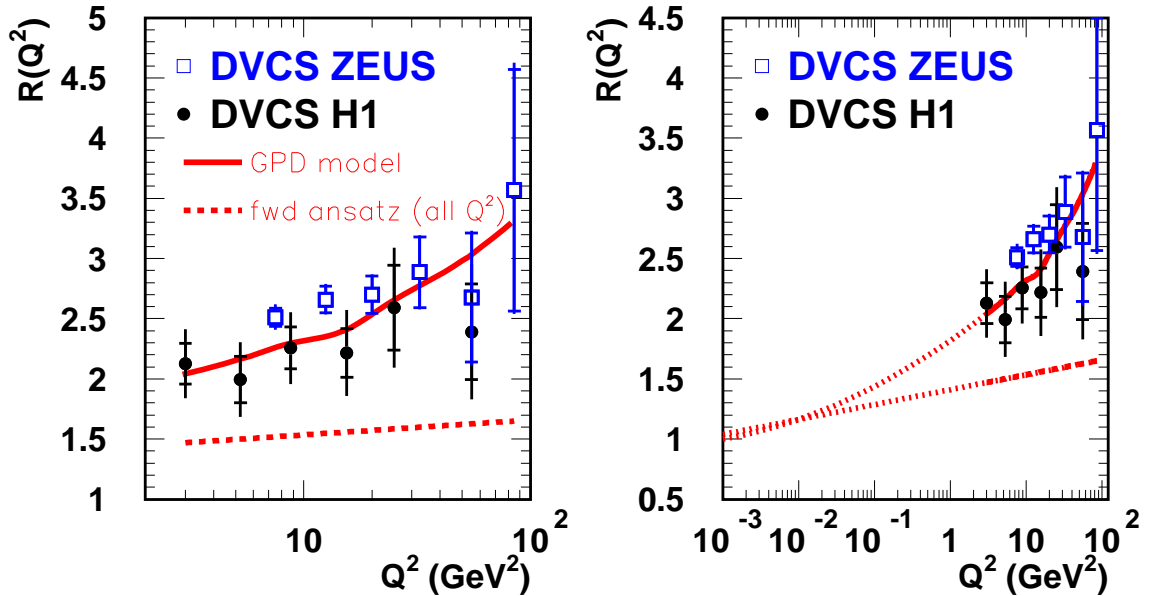


FIG. 4: Skewing factor  $R \equiv \left. \text{Im} \mathcal{A}(\gamma^* + p \rightarrow \gamma + p) \right|_{t=0} / \left. \text{Im} \mathcal{A}(\gamma^* + p \rightarrow \gamma^* + p) \right|_{t=0}$  extracted from DVCS and DIS cross sections as explained in section III. The GPD model is also displayed and gives a good agreement of the data (full line). The forward ansatz model, used at all values of  $Q^2$ , fails to reproduce the total skewing effects generated by the QCD evolution (dashed line) -see text-. On the left, the same skewing factor is presented but with a zoom on the low  $Q^2$  domain. In the limit of vanishing  $Q^2$  values, we expect that the skewing factor tends to unity. The GPD model of section II and the pure forward model described above are then propagated towards very low  $Q^2$  values and we observe the convergence to  $R = 1$  in both cases.

#### IV. BEAM CHARGE ASYMMETRY (BCA) AT HERMES AND COMPASS

The determination of a cross section asymmetry with respect to the beam charge,  $(d\sigma^+ - d\sigma^-)/(d\sigma^+ + d\sigma^-)$ , has been realised by the HERMES experiment [20] for  $x_{Bj} \simeq 0.1$ ,  $Q^2 \simeq 3 \text{ GeV}^2$  and  $|t| < 0.7 \text{ GeV}^2$ . The interest of this measurement lies in its large sensitivity to the shape of the GPD in  $X, \zeta$  [13] and also in the correlations between longitudinal and transverse variables [11].

Using DVCS cross section measurements in the low  $x_{Bj}$  kinematic domain, we have tested with success the GPD model described in section II. In this section, we compare the predictions of this model with the results of HERMES [20], which provides measurements of the  $\cos(\phi)$  amplitude of the BCA, where  $\phi$  is the angle between the plane containing the incoming and outgoing leptons and the plane defined by the virtual and real photon. In Table I, we compare the experimental values to the predictions of the GPD model described in this paper, in case of the factorised exponential  $t$  dependence and in the Regge non-factorised  $t$  behaviour. A table is a good way to present these results as for each  $t$  values, the  $x$  and  $Q^2$  values are different.

Contrary to the DVCS cross section predictions, the calculations presented in Table I are very different in both approaches, factorised and non-factorised  $t$  dependences. Therefore, we confirm that BCA is a very sensitive and discriminating observable to study GPD models. Within the present large experimental errors, as shown in Table I, we can not favor one approach but it is clear that further high precision measurements at COMPASS would be of high significance [21].

In Fig. 5, we compare predictions of our model to simulations of the BCA extraction at COMPASS using a  $\mu$  beam of 100 GeV [4, 21]. We present the comparison for one value of  $Q^2$  (4 GeV<sup>2</sup>) and two values of  $x_{Bj}$  (0.05 and 0.1). When we compute the BCA in the factorised exponential  $t$  dependence approximation, we find values compatible with zero, which are not represented in Fig. 5. We just display the predictions of the model obtained in the non-factorised case. Then, both the  $\cos(\phi)$  and  $\cos(2\phi)$  terms contribute to a significant level to the BCA at COMPASS, as illustrated in Fig. 5. We remark that our predictions do not match with the COMPASS simulation done with the model of Ref. [4], which is another illustration of the large discriminative power of this observable on

$-t$ bin (GeV <sup>2</sup> )	$\langle -t \rangle$ (GeV <sup>2</sup> )	$\langle x_B \rangle$	$\langle Q^2 \rangle$ (GeV <sup>2</sup> )	$A_C^{\cos \phi} \pm \text{stat.} \pm \text{sys.}$	fac. GPD model	non-fac. GPD model
$< 0.06$	0.03	0.08	2.0	$0.024 \pm 0.043 \pm 0.022$	0.060	0.065
$0.06 - 0.14$	0.09	0.10	2.6	$0.020 \pm 0.054 \pm 0.022$	0.058	0.070
$0.14 - 0.30$	0.20	0.11	3.0	$0.071 \pm 0.066 \pm 0.028$	0.050	0.078
$0.30 - 0.70$	0.42	0.12	3.7	$0.377 \pm 0.110 \pm 0.081$	0.012	0.092
$< 0.70$	0.12	0.10	2.5	$0.063 \pm 0.029 \pm 0.028$	0.052	0.072

TABLE I: The  $\cos \phi$  amplitude of the beam–charge asymmetry per kinematic bin in  $-t$  after background correction and the respective average kinematic values. In the last two columns, we give the predictions for the GPD model in the factorised and non-factorised dependences of  $t$ .

GPDs parametrisations.

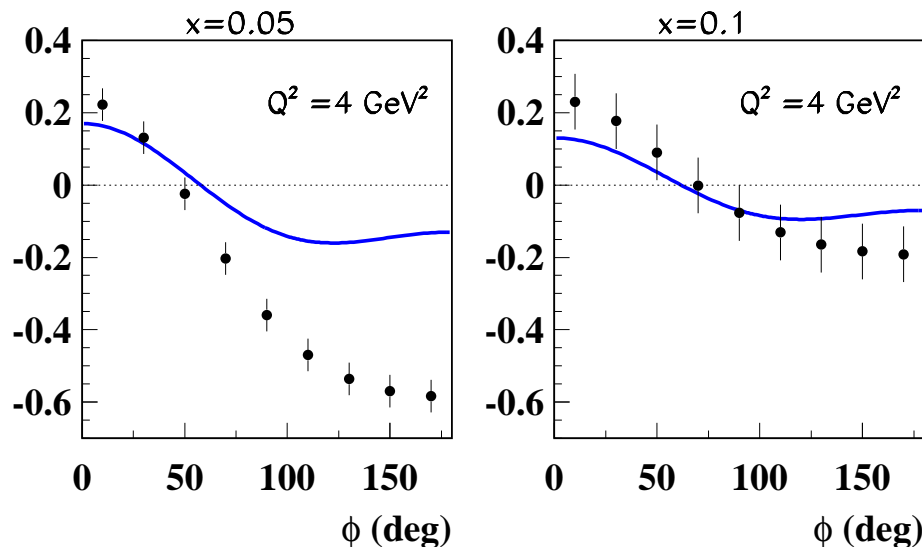


FIG. 5: Simulation of the azimuthal angular distribution of the beam charge asymmetry measurable at COMPASS at  $E_\mu = 100$  GeV. We present the projected values and error bars in the range  $|t| < 0.6$  GeV<sup>2</sup> for 2 values of  $x_{Bj}$  (0.05 and 0.1) at  $Q^2 = 4$  GeV<sup>2</sup> (see Ref. [21]). The prediction of the GPD model with a non-factorised  $t$  dependence is shown (full line). The case of a factorised  $t$  dependence would lead to a prediction of the BCA compatible with zero and is not displayed.

## V. CONCLUSION

An outstanding task in QCD is related to the extraction of GPDs. In contrast to PDFs, these functions contain informations on the correlations between partons, on their transverse motion and thus on the three dimensional structure of the nucleon. Exclusive production of real photon is a prime measurement to access the GPDs, either from DVCS cross section or from BH/DVCS interference. Data are getting more precise, leading to more refinement in the models. In this paper, we have addressed the case of the kinematic domain of HERA. We have shown some basic features, as skewing or  $Q^2$  evolution of GPDs, in a model based on a forward ansatz in the DGLAP region. We have discussed the  $t$  dependence in the factorised and non-factorised approximations. A good agreement of DVCS cross sections from H1 and ZEUS have been obtained in both cases. We have compared this model with success also on the skewing factor  $R \equiv \text{Im} \mathcal{A}(\gamma^* + p \rightarrow \gamma + p)|_{t=0} / \text{Im} \mathcal{A}(\gamma^* + p \rightarrow \gamma^* + p)|_{t=0}$ , which is an interesting quantity as it includes both the non-forward kinematics and the non-diagonal effects. Finally, we have shown that the BCA is certainly the most sensitive observable to the different hypothesis needed in the GPDs parametrisations. We have

shown that the approximations done for the  $t$  dependence lead to significant differences for the predictions in the HERMES kinematic domain, and even larger for COMPASS.

### Acknowledgements

I would like to thank N. d'Hose, P. Guichon and E. Sauvan for useful remarks and comments on the manuscript.

- 
- [1] X. Ji, Phys. Rev. Lett. **78** (1997) 610 [hep-ph/9603249].
  - [2] A.V. Radyushkin, Phys. Rev. D **56** (1997) 5524 [hep-ph/9704207].
  - [3] M. Diehl, T. Gousset, B. Pire and J. P. Ralston, Phys. Lett. B **411** (1997) 193 [hep-ph/9706344].
  - [4] M. Vanderhaeghen, P. A. M. Guichon and M. Guidal, Phys. Rev. D **60** (1999) 094017 [hep-ph/9905372].
  - [5] J. P. Ralston and B. Pire, Phys. Rev. D **66** (2002) 111501 [hep-ph/0110075].
  - [6] A. V. Belitsky, D. Mueller and A. Kirchner, Nucl. Phys. B **629** (2002) 323 [arXiv:hep-ph/0112108].
  - [7] M. Burkardt, Int. J. Mod. Phys. A **18** (2003) 173 [hep-ph/0207047].
  - [8] M. Diehl, Eur. Phys. J. C **25** (2002) 223 [Erratum-ibid. C **31** (2003) 277] [hep-ph/0205208].
  - [9] For a review see *e.g.* M. Diehl, Phys. Rep. **388** (2003) 41, DESY-THESIS-2003-018 [hep-ph/0307382].
  - [10] K. Kumericki, D. Muller and K. Passek-Kumericki, [hep-ph/0703179].
  - [11] V. Guzey and T. Teckentrup, Phys. Rev. D **74** (2006) 054027 [hep-ph/0607099].
  - [12] L. Frankfurt, M. Strikman and C. Weiss, Ann. Rev. Nucl. Part. Sci. **55** (2005) 403 [hep-ph/0507286].
  - [13] A. Freund, Phys. Rev. D **68** (2003) 096006 [hep-ph/0306012].
  - [14] C. Adloff *et al.* [H1 Collaboration], Phys. Lett. B **517** (2001) 47 [hep-ex/0107005].
  - [15] C. Aktas *et al.* [H1 Collaboration], Eur. Phys. J. C **44**, 1-11 (2005), [hep-ex/0505061].
  - [16] S. Chekanov *et al.* [ZEUS collaboration], Phys. Lett. B **573** (2003) 46 [hep-ex/0305028].
  - [17] A. Airapetian *et al.* [HERMES Collaboration], Phys. Rev. Lett. **87** (2001) 182001 [hep-ex/0106068].
  - [18] S. Stepanyan *et al.* [CLAS Collaboration], Phys. Rev. Lett. **87** (2001) 182002 [hep-ex/0107043].
  - [19] C. Munoz Camacho *et al.* [Jefferson Lab Hall A Collaboration], Phys. Rev. Lett. **97** (2006) 262002 [nucl-ex/0607029].
  - [20] A. Airapetian *et al.* [HERMES Collaboration], Phys. Rev. D **75** (2007) 011103 [hep-ex/0605108].
  - [21] N. d'Hose, E. Burtin, P. A. M. Guichon and J. Marroncle, Eur. Phys. J. A **19** (2004) SUPPL147.
  - [22] D. Stump, J. Huston, J. Pumplin, W.-K. Tung, H.L. Lai, S. Kuhlmann and J.F. Owens, JHEP **0310** (2003) 046 [hep-ph/0303013].
  - [23] C. Adloff *et al.* [H1 Collaboration], Eur. Phys. J. C21 (2001) 33-61, [hep-ex/0012053].
  - [24] C. Adloff *et al.* [H1 Collaboration], Phys. Lett. B **520**, 183 (2001), [hep-ex/0108035].